# *In vivo* formation of complex microvessels lined by human endothelial cells in an immunodeficient mouse

**Jeffrey S. Schechner*†‡, Anjali K. Nath*†, Lian Zheng§, Martin S. Kluger*†, Christopher C. W. Hughes¶‖, M. Rocio Sierra-Honigmann¶, Marc I. Lorber**, George Tellides**, Michael Kashgarian¶, Alfred L. M. Bothwell§, and Jordan S. Pober*†§¶**

*Interdepartmental Program in Vascular Biology and Transplantation, Department of †Dermatology, §Section of Immunobiology, and Departments of ¶Pathology and **Surgery, Yale University School of Medicine, New Haven, CT 06536

Communicated by Vincent T. Marchesi, Yale University School of Medicine, New Haven, CT, May 25, 2000 (received for review February 23, 2000)

**We have identified conditions for forming cultured human umbilical vein endothelial cells (HUVEC) into tubes within a three-dimensional gel that on implantation into immunoincompetent mice undergo remodeling into complex microvessels lined by human endothelium. HUVEC suspended in mixed collagen/fibronectin gels organize into cords with early lumena by 24 h and then apoptose. Twenty-hour constructs, s.c. implanted in immunodeficient mice, display HUVEC-lined thin-walled microvessels within the gel 31 days after implantation. Retroviral-mediated overexpression of a caspase-resistant Bcl-2 protein delays HUVEC apoptosis *in vitro* for over 7 days. Bcl-2-transduced HUVEC produce an increased density of HUVEC-lined perfused microvessels *in vivo* compared with untransduced or control-transduced HUVEC. Remarkably, Bcl-2- but not control-transduced HUVEC recruit an ingrowth of perivascular smooth-muscle $\alpha$-actin-expressing mouse cells at 31 days, which organize by 60 days into HUVEC-lined multilayered structures resembling true microvessels. This system provides an *in vivo* model for dissecting mechanisms of microvascular remodeling by using genetically modified endothelium. Incorporation of such human endothelial-lined microvessels into engineered synthetic skin may improve graft viability, especially in recipients with impaired angiogenesis.**

Angiogenesis and vascular remodeling play significant roles in wound healing, tumor growth, cardiovascular disease, and tissue transplantation. Consequently, significant effort has been directed at developing models in which to study and manipulate these processes. Angiogenesis is typified by the elongation of thin-walled capillary tubes from existing vascular structures, followed by investment with mesenchymal cells such as pericytes and smooth-muscle cells during the formation of mature stable vessels (1, 2). Advances in understanding the mechanism of early vascular remodeling have come from the ability to successfully suspend the endothelial cells (EC) in three-dimensional (3D) culture, where they form tubular structures that resemble immature capillaries (3, 4). Such models have been applied to assessing the effects of soluble factors such as vascular endothelial growth factor, leptin, or angiopoietin-1 on vascular remodeling (5–7). These 3D culture systems have been particularly useful in analyzing the interactions between matrix molecules and EC (8, 9).

Reports of models useful for discerning the mechanisms of incorporation of mesenchymal cells into mature vessels have been limited. Coculture of canine-brain EC with astrocytes suspended in a collagen matrix has resulted in the formation of complex vessel-like structures composed of both cell types (10). Other studies on the recruitment and incorporation of pericytes and smooth-muscle cells, although useful in identifying receptor-ligand pairs that may be important in these processes, either have been two-dimensional (11) or have addressed remodeling associated with vasculogenesis during embryonic development rather than angiogenesis in adults (12–14).

Our goal was to construct a synthetic human vascular bed that allows genetic manipulation of endothelial cells to improve perfusion *in vivo.* The aims of such a pursuit are to provide a model for further analysis of the mechanisms of complex vascular organization as well as to develop a stable engineered vascular bed that can be used to perfuse transplanted human tissue. A major limitation in the construction of human synthetic microvessels is apoptosis of cultured human endothelial cells (15). Interaction with matrix components through the integrins $\alpha_5\beta_1$ or $\alpha_v\beta_3$ has been shown to inhibit EC apoptosis in culture (16) and *in vivo* (17). Increased expression of the survival gene Bcl-2 also appears to play a role in preventing the involution of synthetic capillary networks (18). Overexpression of Bcl-2 by retroviral transduction not only resulted in prolonged survival of human dermal microvascular EC but also allowed incorporation of human EC into mouse capillaries *in vivo* (19).

Here we report an optimized methodology for induction of tube formation by cultured human umbilical-vein EC (HUVEC) within 3D gels and for successful inosculation of these preformed networks of cultured cells with the circulatory system of a host. We used severe combined immunodeficient (SCID)/beige immunoincompetent mice to avoid immunologic rejection. A simple extracellular matrix composed of type I collagen plus human plasma fibronectin was used. The survival of and tube formation by cultured HUVEC in such constructs were improved by transduction with a modified (caspase-resistant) form of Bcl-2 protein (20). Such cultured HUVEC are consistently incorporated into the mouse circulatory system. Furthermore, overexpression of Bcl-2 in these cells results in the formation of perfused vascular structures invested by mouse pericyte/smooth-muscle cells that remodel into mature vessels.

## Materials and Methods

**Transduction of HUVEC.** The Bcl-2 retroviral vector was constructed as described elsewhere (21) by using the D34A caspase resistant form of Bcl-2 in the pSG5 expression vector (20) (M. Hardwick, Johns Hopkins University, Baltimore, MD). Stable transduction of HUVEC was achieved by repetitive infections of

Abbreviations: EC, endothelial cells; 3D, three-dimensional; HUVEC, human umbilical-vein endothelial cells; UEA-1, *Ulex europaeus* agglutinin-1; SCID, severe combined immunodeficient; EGFP, enhanced green fluorescent protein.

‡To whom reprint requests should be addressed at: Department of Dermatology, Yale University School of Medicine, P.O. Box 208059, New Haven, CT 06520-8059. E-mail: Jeffrey.Schechner@yale.edu.

‖Present address: Department of Molecular Biology and Biochemistry, University of California, Irvine, CA 92697.

The publication costs of this article were defrayed in part by page charge payment. This article must therefore be hereby marked "*advertisement*" in accordance with 18 U.S.C. §1734 solely to indicate this fact.

Article published online before print: *Proc. Natl. Acad. Sci. USA*, 10.1073/pnas.150242297. Article and publication date are at www.pnas.org/cgi/doi/10.1073/pnas.150242297

HUVEC by using supernatants produced by the packaging cell line (Phoenix Ampho, provided by G. P. Nolan, Stanford University) without drug selection. Daily viral infections were repeated four to six times in the presence of polybrene (5 $\mu$g/ml) in DMEM (GIBCO) until the percentage of cells expressing enhanced green fluorescent protein (EGFP) or Bcl-2 was 97–98%.

**Formation of Vascular Construct.** HUVEC were isolated and cultured as described (22) and were suspended in a solution of rat-tail type 1 collagen (1.5 mg/ml) and human plasma fibronectin (90 $\mu$g/ml) (both from Collaborative Biomedical Products, Bedford, MA) in 25 mM Hepes and 1.5 mg/ml $NaHCO_3$ buffered Medium 199 (Sigma) at 4°C. pH was adjusted to 7.5 by using 0.1 M HCl (Sigma). The HUVEC suspension was pipetted into rat-tail type 1 collagen-coated C-6 transwells (Collaborative Biomedical Products) and warmed to 37°C for 10 min to allow polymerization of the collagen. Warmed Medium 199 supplemented with 20% FBS/50 $\mu$g/ml EC growth factor/200 units/ml penicillin/200 $\mu$g/ml streptomycin/2 mM L-glutamine (all from GIBCO)/100 $\mu$g/ml heparin (Sigma) was added to the transwells to cover the solidified gels. In some experiments, the gels were maintained in culture for as long as 7 days without further growth supplementation. For implantation into animals, gels were harvested and trisected approximately 20 h after formation. Each resulting $1 \times 1 \times 0.2$ cm gel segment was implanted into a bluntly dissected s.c. pouch in the anterior abdominal wall of a 5- to 8-week-old SCID/beige mouse (Taconic Farms). The wound was closed with skin staples. At the time indicated in the text, typically 31 or 60 days, the constructs were harvested and analyzed by conventional histology, immunohistochemistry, and/or electron microscopy.

**Immunocytochemistry.** Double-antibody staining was performed on 4-$\mu$m-thick frozen sections with anti-smooth-muscle $\alpha$-actin mAb (1A4, Sigma) and biotinylated *Ulex europaeus* agglutinin I (UEA-I, Vector Laboratories) by using standard detection techniques (23). Single-antibody staining was performed on 3-$\mu$m-thick formalin-fixed paraffin-embedded sections by using anti-Bcl-2 (124; Dako), anti-human CD31 (JC/70A; Dako), anti-mouse CD31 (Mec 13.3; Becton Dickinson PharMingen), anti-smooth-muscle $\alpha$-actin mAbs, or UEA-1 lectin, followed by a light hematoxylin stain. Isotype-matched nonbinding antibodies were used in all antibody-staining experiments to control for nonspecific reactivity.

**Electron Microscopy.** Tissue was fixed in Karnovsky's fixative and processed as described (24). For *in vivo* experiments, cardiac perfusion with the fixative was performed on anesthetized animals. Sections were viewed on a Zeiss EM 910 electron microscope at 80 kV.

**Data Collection and Statistical Analysis.** The number of vessels per area of gel was calculated by dividing the number of endothelial-lined spaces that contained erythrocytes within the entire gel in hematoxylin/eosin-stained formalin-fixed tissue sections by the cross-sectional area of the gel. An observer blinded to treatment protocol counted the vascular profiles. The cross-sectional area of the gels was obtained from video microscopy images by using NIH IMAGE software. All specimens were stained with UEA-1 to ensure that greater than 99% of the vascular profiles were lined by human endothelium. Statistical analyses of significance were performed by using a paired *t*-test.

## Results

HUVEC rapidly undergo apoptosis when suspended in type I collagen gels (ref. 15 and unpublished observations). Therefore, our initial studies were aimed at delaying apoptosis by suspending early-passage HUVEC in a mixed collagen-fibronectin gel, combining the structural properties of type I collagen fibers with the cell adhesive and survival enhancing properties of fibronectin (16, 25). By 18 h in this gel culture, isolated HUVEC spontaneously reorganized into multicellular cords (Fig. 1*a*) and by 24 h these cords appeared to be in the early stages of developing lumena free of collagen fibers (Fig. 1*b*). However, by 24 h significant numbers of EC showed morphologic evidence of apoptosis (Fig. 1*c*), and by 48 h, essentially all of the HUVEC had died.

We s.c. implanted 20-h HUVEC-derived synthetic "vascular beds" into 11 SCID/beige mice. Constructs harvested 31 days after implantation contained thin-walled tubes filled with erythrocytes, consistent with perfusion by the mouse circulation (Fig. 1*d*). These vascular profiles were present in 10 of the 11 constructs at a mean density of $124.1 \pm 2.8$ per $10^5$ $\mu m^2$. As assessed by UEA-1 lectin staining, the majority of tubes were wholly composed of human EC (Fig. 1*e*). In contrast, anti-mouse CD31 antibodies reacted with fewer than 1% of the vascular profiles (data not shown) within the constructs, confirming that the vessel-like structures were not formed by mouse neovascularization of the gel. Vascular profiles failed to develop if the HUVEC did not form cords before implantation, and early-passage level HUVEC were consistently superior to those at later passage in forming perfused vascular profiles *in vivo* (data not shown). In mock constructs, which contained no HUVEC, there were no detectable vascular profiles except at the very edges of these empty collagen gels 31 days after implantation (Fig. 1 *f* and *g*). We conclude that HUVEC-derived cords formed *in vitro* survive, evolve into tubes, and inosculate with mouse microvessels at the gel boundary, acquiring perfusion.

Because apoptosis limited cord formation *in vitro*, we evaluated whether further inhibition of apoptosis would improve the performance of the synthetic microvessel constructs. We recently described retroviral transduction of an exogenous Bcl-2 protein, mutated to resist caspase-mediated inactivation, into early passage HUVEC at high efficiency without drug selection (21). We compared EGFP-transduced HUVEC controls with Bcl-2-transduced cells in our synthetic vessel system. When cultured in a collagen/fibronectin gel for 24 h, both the EGFP- and Bcl-2-transduced cells readily form into cords similar in appearance to nontransduced HUVEC (Fig. 2 *a* and *b*). EGFP-transduced HUVEC display green autofluorescence 24 h after incorporation into the constructs, indicating expression of EGFP (Fig. 2*c*), whereas immunohistochemistry confirmed the expression of the Bcl-2 transgene in Bcl-2-transduced cells (Fig. 2*d*). By 36 h in gel culture, few intact EGFP-transduced HUVEC tubes remained (Fig. 2*e*), whereas those formed from Bcl-2-transduced HUVEC continued to elongate (Fig. 2*f*). By day 7 in culture, no viable EGFP-transduced HUVEC were detectable (Fig. 2*g*), whereas the Bcl-2-transduced EC maintained capillary-like structures ($n = 3$, Fig. 2*h*). Thus, Bcl-2 overexpression effectively increased the persistence of HUVEC-derived cords in collagen/fibronectin gel culture.

Ten mice were implanted with 18- to 24-h vascular constructs containing EGFP-transduced and 11 with Bcl-2-transduced HUVEC. By 31 days after implantation into mice, transduced HUVEC constructs developed perfused human endothelial-lined vascular profiles (Fig. 3 *a–d*), and the tubular structures maintained expression of the transduced gene products *in vivo* (Fig. 3 *e* and *f*). Murine vessels did not significantly contribute to these vascular beds (Fig. 3*g*). However, there were several striking morphologic differences between Bcl-2- and EGFP-transduced vascular constructs. Overexpression of Bcl-2 significantly increased the density of vascular structures to an average of $431.5 \pm 19.9$, compared with $81.5 \pm 22.6$ vascular profiles per $10^4$ $\mu m^2$ in the EGFP group ($P = 1.6 \times 10^{-7}$). The endothelial-lined structures formed from Bcl-2-overexpressing cells showed

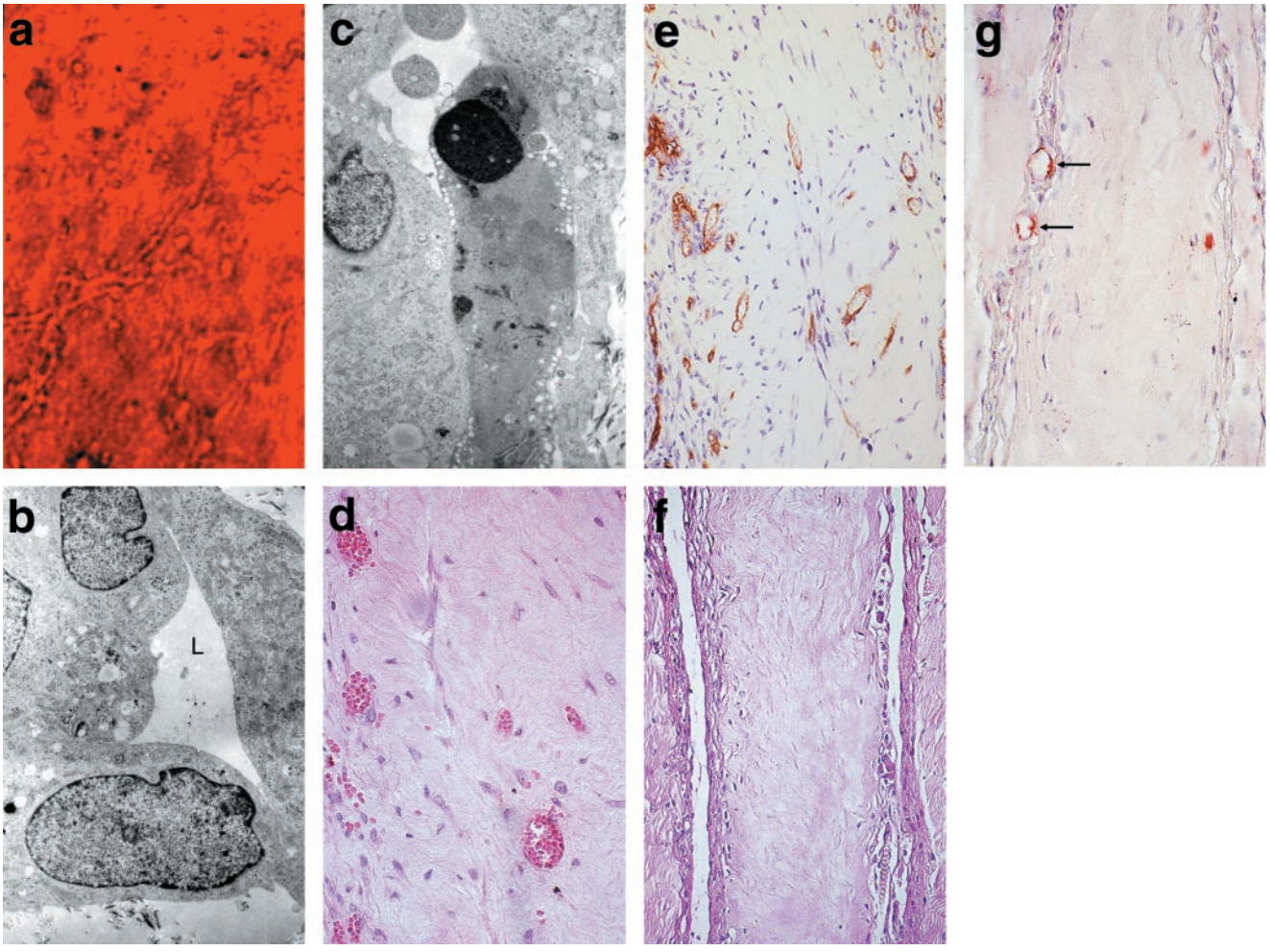


**Fig. 1.** The behavior of HUVEC in 3D-gel culture and in synthetic vascular beds *in vivo*. (*a*) Phase-contrast microscopy of HUVEC in 3D-gel culture 24 h after suspension in a collagen fibronectin gel (×400). (*b*) Electron microscopy (EM) of these constructs showing the HUVEC form aggregates with a lumen-like (L, lumen) configuration cleared of matrix proteins (×10,000). (*c*) EM of another field of the same construct containing a cell undergoing apoptosis as demonstrated by condensation of the nucleus (×10,000). (*d*) HUVEC construct harvested 31 days after implantation into a SCID/beige mouse [hematoxylin/eosin (H + E) stain, ×400]. (*e*) UEA-1 reactivity is seen on the cells lining the vascular spaces (×200). (*f*) Mock construct in which HUVEC were not included in the gel (H + E stain, ×200). (*g*) Anti-murine CD31 reactivity (red) limited to the edges of the specimen shown in *f* (arrows, ×400). All magnifications are reported as original magnification before photographic enlargement.

a much greater variation in size and shape, with visible branching, than those formed from EGFP-transduced cells (Fig. 3 *a* and *b*). In addition, many of the vascular structures lined by Bcl 2-transduced HUVEC appeared to have two or more cell layers. The inner layer was composed of Bcl-2-, UEA-1-, and human CD31-expressing human endothelial cells, but the outer investing layers were UEA-1, CD31, and Bcl-2 negative and smooth-muscle $\alpha$-actin positive (Fig. 4 *a–d*). No myosin thick filaments were detected in these investing cells by electron microscopy, consistent with their identity as pericytes or incompletely differentiated vascular smooth-muscle cells (Fig. 5 *a–c*). These investing cells appear to have been recruited from the surrounding mouse tissue, because the density of extravascular cells was greatest at the periphery of the constructs, especially evident in a limited number of specimens harvested only 14 days after implantation. Similar structures were not observed in any of the constructs transduced with EGFP or in those of previous experiments by using HUVEC that had not been transduced. Seven additional constructs containing Bcl-2-transduced cells were harvested 60 days after implantation. In six of these specimens, the HUVEC-lined vascular structures were organized into complex vascular beds with elements that closely resembled arterioles, venules, and capillaries (Fig. 4 *e* and *f*). Using the same immunohistochemical analyses applied at 30 days, we found that these vessels were comprised of HUVEC surrounded by supporting cells of mouse origin. Thus, Bcl-2 transduction promotes both HUVEC survival and enhanced vascular remodeling, resulting in the formation of mature vascular beds.

## Discussion

In the present study, we developed a model for the routine introduction of HUVEC into a synthetic vascular bed to test whether genetic modification of human EC can enhance vascular remodeling, with the ultimate aim of forming a stable vascular bed suitable for perfusing tissue equivalents. The overexpression of a survival gene known to improve capillary tube formation revealed an effect of Bcl-2 on the enhancement of maturation of newly formed vessels.

To ensure that our findings could be applied to the design of engineered tissues, we chose to use HUVEC, which can be routinely cultured in large numbers from a readily available supply of discarded tissue. The collagen–fibronectin matrix we used is similar to that currently found in tissue substitutes

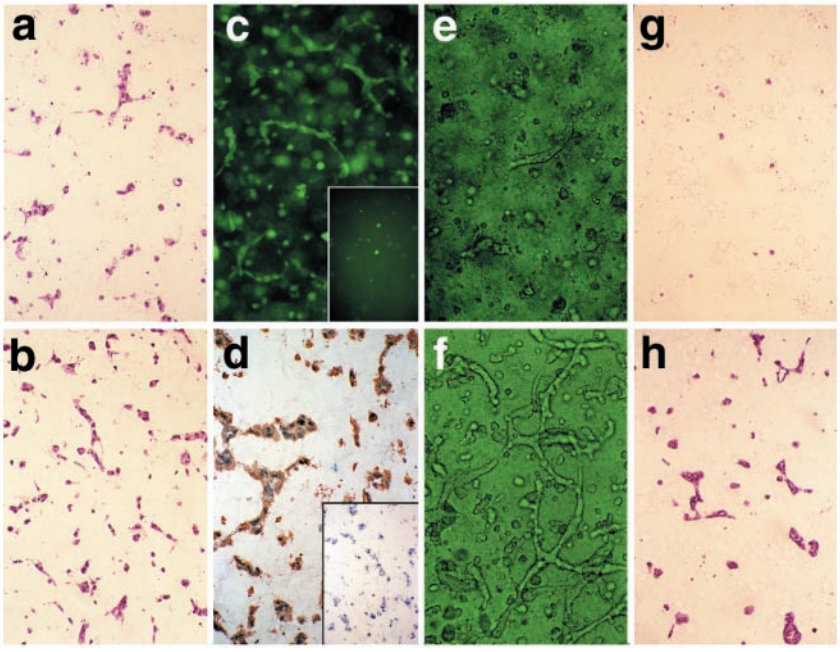


**Fig. 2.** The behavior of retrovirally transduced HUVEC *in vitro*. H + E staining of (*a*) EGFP- and (*b*) Bcl-2-transduced HUVEC, 24 h after suspension in 3D-gel culture (×200). (*c*) Intrinsic fluorescence of an EGFP-transduced [and (*Inset*) absence of signal from Bcl-2-transduced] HUVEC construct (×100). (*d*) Anti-Bcl-2 antibody staining of the Bcl-2-transduced [brown and (*Inset*) EGFP-transduced] construct at this same time point (×200). (*e* and *f*) Phase-contrast microscopy of the EGFP- (*e*) and Bcl-2- (*f*) transduced HUVEC maintained in 3D-gel culture for 36 h (×400). After 7 days in 3D-gel culture, there are no detectable viable EGFP-transduced cells (*g*), whereas those transduced with Bcl-2 are still organized into cords (*h*) (×400).

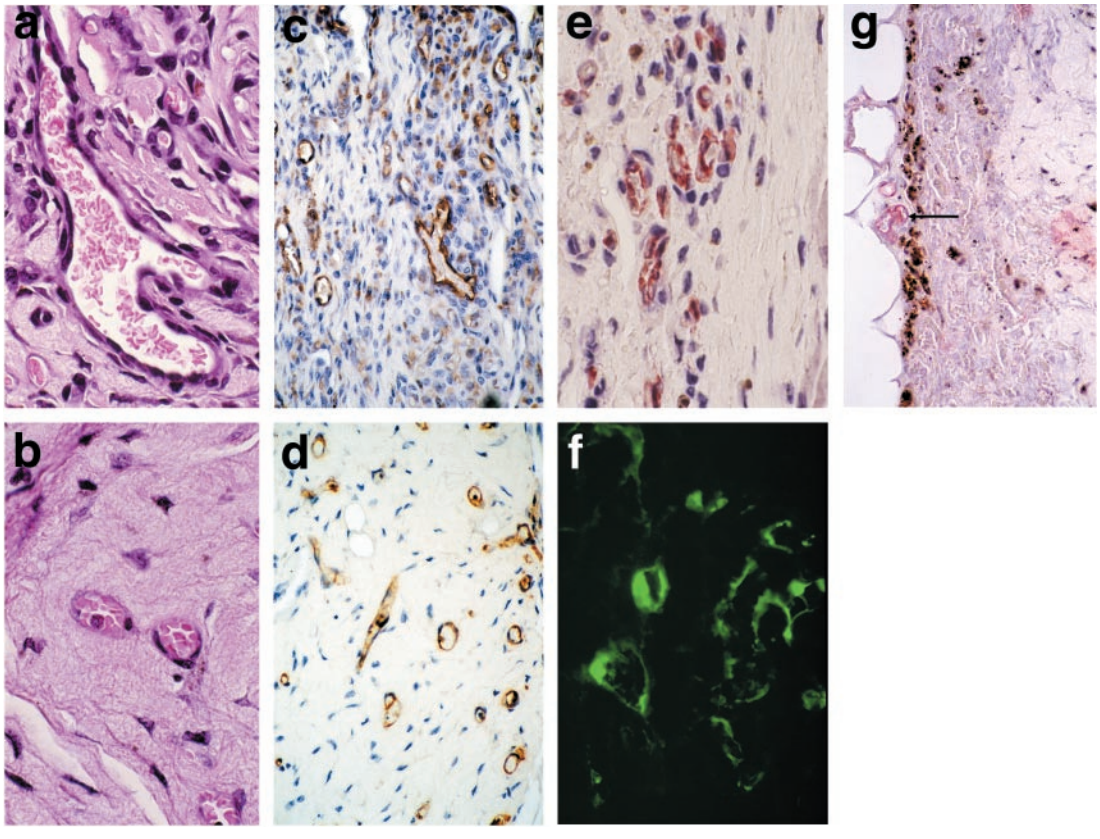


**Fig. 3.** The behavior of retrovirally transduced HUVEC *in vivo*. Histology of (*a*) Bcl-2- and (*b*) EGFP-transduced HUVEC constructs harvested 31 days after implantation into a SCID/beige mouse (×1,000). UEA-1 staining (brown) of the constructs in *a* (*c*) and *b* (*d*) (×200). (*e*) Anti-Bcl-2 staining (brown) of a Bcl-2-transduced construct 31 days after implantation into a SCID/beige mouse (×1,000). (*f*) Fluorescence of the EGFP-transduced HUVEC constructs *in vivo* (×400). (*g*) Anti-murine CD31 staining (red) of a Bcl-2-transduced HUVEC construct *in vivo*, showing the restriction of mouse microvessels to the edge of the construct (arrow, ×400).

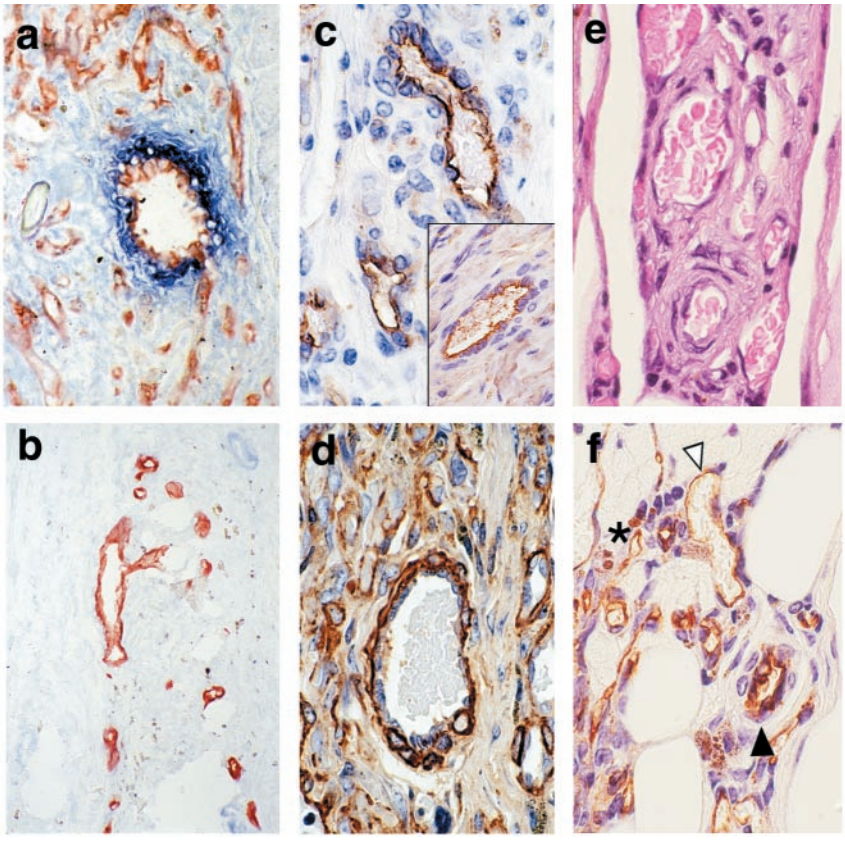


**Fig. 4.** Analysis of complex vascular structures. Double immunostaining of frozen sections for UEA-1 (red) and smooth-muscle $\alpha$-actin (blue) in (*a*) BCL-2- and (*b*) EGFP-transduced constructs harvested from mice 31 days after implantation ($\times$200). (*c*) UEA-1 staining (*Inset*, anti-human CD31, both shown in brown) of a larger vessel from a Bcl-2-transduced construct 31 days after implantation ($\times$400). (*d*) Smooth-muscle $\alpha$-actin staining (brown) of this same construct ($\times$400). (*e*) Histology of a Bcl-2-transduced construct harvested 60 days after implantation. (*f*) UEA-1 staining (brown) of this same construct (▶, arteriole-like structure; ◁, venule-like structure; *, capillary-like structure; $\times$400).

available for clinical usage (26). This matrix supported the organization of HUVEC into primitive capillary-like structures by 18 to 24 h in culture and led to the development of human EC-lined microvessels perfused by the mouse circulation after implantation. No significant mouse neovascularization or inflammation was associated with these constructs, indicating that a suitable balance had been achieved between sustaining human vessels and minimizing the host response.

We demonstrated that a high-efficiency retroviral transduction technique can result in the persistent expression of a transgene in human EC that are perfused by the host circulation. The overexpression of Bcl-2 had the expected effect of increasing the density of the vascular bed, but surprisingly also enhanced vascular remodeling. Specifically, we observed the development of larger vessels, with increased branching, invested with additional cellular layers, and surrounded by more numerous inter-

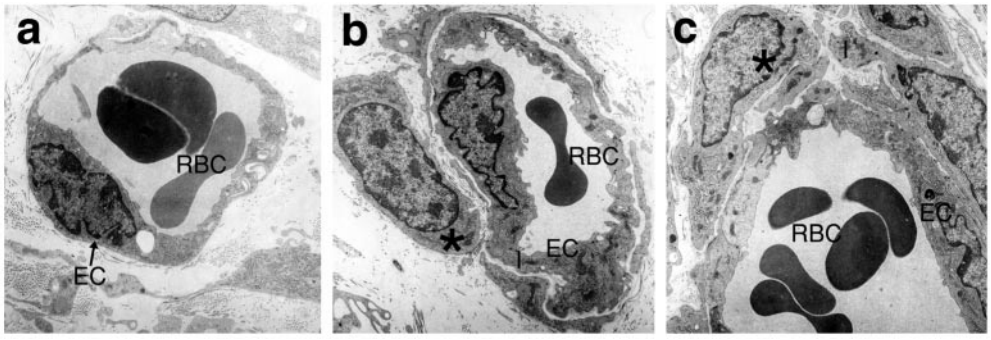


**Fig. 5.** Electron microscopy of constructs 31 days after implantation into SCID/beige mice. (*a*) Untransduced HUVEC have formed perfused vessel-like structures that have inosculated with the mouse circulation, as demonstrated by the presence of erythrocytes within the lumen. The vessel has a single endothelial layer surrounded by matrix. (*b*) The Bcl-2-transduced HUVEC have formed more complex vessels that are now comprised of the EC layer surrounded by a second layer representing a pericyte/smooth-muscle cell. (*c*) This vessel, formed from Bcl-2-transduced HUVEC, shows an even more complex structure with an endothelial layer surrounded by several layers of investing cells, mimicking the anatomy of a postcapillary venule. (RBC, erythrocytes; *, investing cell; EC, endothelial cell; $\times$10,000).

stitial cells. In animals in which the remodeling was allowed to continue for 60 days, the resultant vascular structures actually appeared to represent small arterioles, venules, and capillaries. Although the identity of the investing cells could not be definitively established by electron microscopy, the smooth-muscle $\alpha$-actin positivity and the ''boxcar'' oval nuclei are consistent with their being pericytes or incompletely differentiated smooth-muscle cells. These investing cells are almost certainly of murine origin, because unlike the cells initially incorporated in the construct, they were Bcl-2 and UEA-1 negative. The mechanism by which Bcl-2 overexpression in HUVEC results in recruitment of mesenchymal cells and the formation of multilayered vascular structures is not clear. It is unlikely that this finding is simply caused by an increased number of surviving HUVEC producing a greater quantity of a recruitment signal, because there were occasional specimens in which the number of untransduced or control EGFP-transduced vascular profiles equaled or exceeded those typically found in the Bcl-2-transduced HUVEC constructs, yet only thin-walled capillary-like structures were observed. A more likely explanation is that Bcl-2 itself, which is not normally expressed by HUVEC, turns on production of a recruitment signal. The identity of the putative mesenchymal cell recruitment signal(s) is under investigation. Evidence from studies of embryonic vasculogenesis and vascular remodeling in animal models suggests that the likely candidates known to be produced by EC include vascular endothelial growth factor (14, 27), platelet-derived growth factor (11, 28), angiopoietin-1 (29), and/or heparin-binding epidermal growth factor (30).

It has been proposed that investment of newly formed capillary tubes with pericytes is necessary to maintain their integrity. Therefore, we believe that incorporation of similar vascular beds formed from endothelial cells that overexpress Bcl-2 into engineered tissues is likely to greatly improve their clinical utility. In the early posttransplant period before host neovascularization, transplanted tissues are wholly dependent on diffusion for survival (31). Clinical experience with synthetic skins indicates that the absence of early perfusion may significantly limit successful engraftment, especially when implanted into compromised recipient beds (e.g., in diabetes, thermal burns, or venous leg ulcers) (32, 33), or in hosts with impaired angiogenesis (e.g., the elderly).

There are potential hazards to incorporation of EC that have undergone retroviral transduction into synthetic tissues intended for human use. First, the possibility of producing infectious retrovirus is a concern that has been significantly minimized, or even eliminated, by using a packaging cell system that cannot incorporate viral replication genes into the vector (34). Another concern is that the target cell may undergo malignant transformation. *In vitro* experiments (21) have shown that Bcl-2-transduced HUVEC show no evidence of transformation in culture, and we found no evidence of tumor formation or invasion of mouse tissue by Bcl-2-transduced cells 90 days after implantation *in vivo*. The safety of these manipulations will require further evaluation, but there are no indications to date that suppression of apoptosis in endothelium is by itself tumorigenic.

In summary, we have developed a reliable method for incorporation of normal or genetically altered human EC into a synthetic tissue-like structure. Our finding that Bcl-2 overexpression enhances the formation of complex vascular structures opens the possibility of using this model to study vascular remodeling. When applied to engineered tissues, a method for the development of a mature vascular bed is likely to improve the viability of tissue equivalents, especially when engrafting them into a compromised recipient bed.

This work was supported in part by National Institutes of Health Grants R01 HL510144 (J.S.P.) and R01 HL51448 (A.L.M.B.), the Yale Skin Diseases Research Core Center (P30 AR4192), and a Dermatology Foundation Clinical Career Development Award (J.S.S.).

1. Risau, W. (1997) *Nature (London)* **386,** 671–674.
2. Hanahan, D. (1997) *Science* **277,** 48–50.
3. Springhorn, J. P., Madri, J. A. & Squinto, S. P. (1995) *In Vitro Cell Dev. Biol. Anim.* **31,** 473–481.
4. Madri, J. A. & Marx, M. (1992) *Kidney Int.* **41,** 560–565.
5. Papapetropoulos, A., Garcia-Cardena, G., Madri, J. A. & Sessa, W. C. (1997) *J. Clin. Invest.* **100,** 3131–3139.
6. Sierra-Honigmann, M. R., Nath, A. K., Murakami, C., Garcia-Cardena, G., Papapetropoulos, A., Sessa, W. C., Madge, L. A., Schechner, J. S., Schwabb, M. B., Polverini, P. J., *et al.* (1998) *Science* **281,** 1683–1686.
7. Papapetropoulos, A., Garcia-Cardena, G., Dengler, T. J., Maisonpierre, P. C., Yancopoulos, G. D. & Sessa, W. C. (1999) *Lab. Invest.* **79,** 213–223.
8. Merwin, J. R., Anderson, J. M., Kocher, O., Van Itallie, C. M. & Madri, J. A. (1990) *J. Cell Physiol.* **142,** 117–128.
9. Sankar, S., Mahooti-Brooks, N., Bensen, L., McCarthy, T. L., Centrella, M. & Madri, J. A. (1996) *J. Clin. Invest.* **97,** 1436–1446.
10. Ment, L. R., Stewart, W. B., Scaramuzzino, D. & Madri, J. A. (1997) *In Vitro Cell Dev. Biol. Anim.* **33,** 684–691.
11. Hirschi, K. K., Rohovsky, S. A., Beck, L. H., Smith, S. R. & D'Amore, P. A. (1999) *Circ. Res.* **84,** 298–305.
12. Thurston, G., Suri, C., Smith, K., McClain, J., Sato, T. N., Yancopoulos, G. D. & McDonald, D. M. (1999) *Science* **286,** 2511–2514.
13. Sato, T. N., Tozawa, Y., Deutsch, U., Wolburg-Buchholz, K., Fujiwara, Y., Gendron-Maguire, M., Gridley, T., Wolburg, H., Risau, W. & Qin, Y. (1995) *Nature (London)* **376,** 70–74.
14. Shalaby, F., Rossant, J., Yamaguchi, T. P., Gertsenstein, M., Wu, X. F., Breitman, M. L. & Schuh, A. C. (1995) *Nature (London)* **376,** 62–66.
15. Ilan, N., Mahooti, S. & Madri, J. A. (1998) *J. Cell Sci.* **111,** 3621–3631.
16. Fukai, F., Mashimo, M., Akiyama, K., Goto, T., Tanuma, S. & Katayama, T. (1998) *Exp. Cell Res.* **242,** 92–99.
17. Brooks, P. C., Montgomery, A. M., Rosenfeld, M., Reisfeld, R. A., Hu, T., Klier, G. & Cheresh, D. A. (1994) *Cell* **79,** 1157–1164.
18. Pollman, M. J., Naumovski, L. & Gibbons, G. H. (1999) *J. Cell Physiol.* **178,** 359–370.
19. Nor, J. E., Christensen, J., Mooney, D. J. & Polverini, P. J. (1999) *Am. J. Pathol.* **154,** 375–384.
20. Cheng, E. H., Kirsch, D. G., Clem, R. J., Ravi, R., Kastan, M. B., Bedi, A., Ueno, K. & Hardwick, J. M. (1997) *Science* **278,** 1966–1968.
21. Zheng, L., Dengler, T. J., Kluger, M., Madge, L. A., Schechner, J. S., Maher, S. E., Pober, J. S. & Bothwell, A. L. M. (2000) *J. Immunol.* **164,** 4665–4671.
22. Gimbrone, M. A., Jr. (1976) *Prog. Hemost. Thromb.* **3,** 1–28.
23. Schechner, J. S., Edelson, R. L., McNiff, J. M., Heald, P. W. & Pober, J. S. (1999) *Lab. Invest.* **79,** 601–607.
24. Slowik, M. R., De Luca, L. G., Min, W. & Pober, J. S. (1996) *Circ. Res.* **79,** 736–747.
25. Maciag, T., Kadish, J., Wilkins, L., Stemerman, M. B. & Weinstein, R. (1982) *J. Cell Biol.* **94,** 511–520.
26. Phillips, T. J. (1998) *Arch. Dermatol.* **134,** 344–349.
27. Fong, G. H., Rossant, J., Gertsenstein, M. & Breitman, M. L. (1995) *Nature (London)* **376,** 66–70.
28. Hellstrom, M., Kal n, M., Lindahl, P., Abramsson, A. & Betsholtz, C. (1999) *Development (Cambridge, U.K.)* **126,** 3047–3055.
29. Suri, C., McClain, J., Thurston, G., McDonald, D. M., Zhou, H., Oldmixon, E. H., Sato, T. N. & Yancopoulos, G. D. (1998) *Science* **282,** 468–471.
30. Swinscoe, J. C. & Carlson, E. C. (1992) *J. Cell Sci.* **103,** 453–461.
31. Young, D. M., Greulich, K. M. & Weier, H. G. (1996) *J. Burn Care Rehab.* **17,** 305–310.
32. Grey, J. E., Lowe, G., Bale, S. & Harding, K. G. (1998) *J. Wound Care* **7,** 324–325.
33. Falanga, V., Margolis, D., Alvarez, O., Auletta, M., Maggiacomo, F., Altman, M., Jensen, J., Sabolinski, M. & Hardin-Young, J. (1998) *Arch. Dermatol.* **134,** 293–300.
34. Pear, W. S., Nolan, G. P., Scott, M. L. & Baltimore, D. (1993) *Proc. Natl. Acad. Sci. USA* **90,** 8392–8396.